

Review

# Conductive Polymer and Nanoparticle-Promoted Polymer Hybrid Coatings for Metallic Bipolar Plates in Proton Membrane Exchange Water Electrolysis

Gaoyang Liu <sup>1,2,\*</sup>, Faguo Hou <sup>1,2</sup>, Xindong Wang <sup>1,2</sup> and Baizeng Fang <sup>1,2,\*</sup>

<sup>1</sup> Department of Energy Storage Science and Technology, University of Science and Technology Beijing, 30 College Road, Beijing 100083, China

<sup>2</sup> Department of Metallurgical and Ecological Engineering, University of Science and Technology Beijing, 30 College Road, Beijing 100083, China

\* Correspondence: liugy@ustb.edu.cn (G.L.); baizengfang@163.com (B.F.)

**Abstract:** Proton exchange membrane water electrolysis (PEMWE) is a green hydrogen production technology with great development prospects. As an important part of PEMWE, bipolar plates (BPs) play an important role and put forward special requirements due to the harsh environments on both the anode and cathode. Recently, metal-based BPs, particularly stainless steel and titanium BPs have attracted much attention from researchers all over the world because of their advantages of high corrosion resistance, low resistivity, high thermal conductivity, and low permeability. However, these metallic BPs are still prone to being oxidized and are facing with hydrogen embrittlement problems in the PEMWE working environment, which would result in reduced output power and premature failure of the PEMWE stack. In order to reduce the corrosion rate and maintain low interfacial contact resistance, the surface modification of the metallic BPs with protective coatings, such as precious metals (e.g., Au, Pt, etc.) and metal nitrides/carbides, etc., have been extensively investigated. However, the above-mentioned coating materials are restricted by the high-cost materials, complex equipment, and the complicated operation process. In this review, the surface modification of metallic BPs based on silane treatment, conductive polymers, e.g., polyaniline (PANI) and polypyrrole (PPy) as well as some nanoparticles-promoted polymer hybrid coatings which have been investigated for PEMWE, are summarized and reviewed. As for the silane treatment, the dense silane can not only effectively enhance the corrosion resistance but also improve the adhesion between the substrate and the conductive polymers. As for PANI and PPy, the typical value of corrosion current density of a PANI coating is  $5.9 \mu\text{A cm}^{-2}$ , which is significantly lower than  $25.68 \mu\text{A cm}^{-2}$  of the bare metal plate. The introduction of nanosized conductive particles in PANI can further reduce the corrosion current density to  $0.15 \mu\text{A cm}^{-2}$ . However, further improvement in the electrical conductivity is still desired to decrease the interface contact resistance (ICR) to be lower than  $10 \text{ m}\Omega \text{ cm}^2$ . In addition, serious peeling off of the coating during long-term operation also needs to be solved. Typically, the conductive polymer reinforced by graphene, noble metals, and their compounds in the form of nanoparticle-promoted polymer hybrid coatings could be a good choice to obtain higher corrosion resistance, durability, and conductivity and to extend the service life of PEMWE. Especially, nanoparticle-promoted polymer hybrid coatings consisting of polymers and conductive noble metals or nitrides/carbides can be controlled to balance the conductivity and mechanical properties. Due to the advantages of a simple preparation process, low cost, and large-scale production, nanoparticle-promoted polymer hybrid coatings have gradually become a research hotspot. This review is believed to enrich the knowledge of the large-scale preparation process and applications of BPs for PEMWE.

**Keywords:** proton exchange membrane water electrolysis; bipolar plates; conductive polymer; inorganic nanoparticles; coatings; corrosion resistance; contact resistance



**Citation:** Liu, G.; Hou, F.; Wang, X.; Fang, B. Conductive Polymer and Nanoparticle-Promoted Polymer Hybrid Coatings for Metallic Bipolar Plates in Proton Membrane Exchange Water Electrolysis. *Appl. Sci.* **2023**, *13*, 1244. <https://doi.org/10.3390/app13031244>

Academic Editor: Philippe Lambin

Received: 23 December 2022

Revised: 11 January 2023

Accepted: 13 January 2023

Published: 17 January 2023

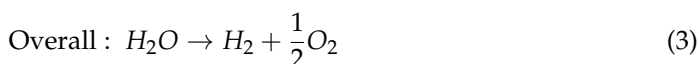
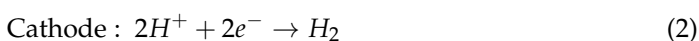
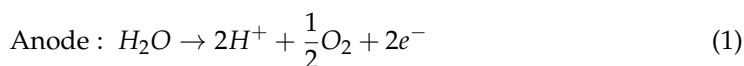


**Copyright:** © 2023 by the authors. Licensee MDPI, Basel, Switzerland. This article is an open access article distributed under the terms and conditions of the Creative Commons Attribution (CC BY) license (<https://creativecommons.org/licenses/by/4.0/>).

## 1. Introduction

Hydrogen is one of the most promising clean and sustainable energy carriers. Generally, the current hydrogen production technologies mainly include *steam* reforming of fossil fuel or biomass gasification, methanol-reforming, an industrial by-product, and water splitting by electrolysis or photocatalysis [1–10]. At present, the process of hydrogen production by water electrolysis has the potential to utilize the fluctuant power generated with renewable energy. Hydrogen and oxygen can be obtained by splitting water with the advantages of environmental friendliness and high purity (99.999%) [11–17]. Among them, proton exchange membrane water electrolysis (PEMWE) using pure water as a reactant has the advantages of low hydrogen permeability, high purity of hydrogen generated, and only removing water vapor [18–21]. In addition, the PEMWE adopts a zero spacing structure with low ohmic resistance, which can significantly improve the overall efficiency of the electrolysis process. Furthermore, it is compact and flexible in operation, which can overcome the uncertainty and volatility in the process of renewable energy power generation [22]. Additionally, the pressure of PEMWE can be adjusted and controlled in a wide range, and the hydrogen output pressure can reach several MPa, which can adapt to the rapidly changing renewable energy power input [23]. Therefore, PEMWE is a green hydrogen production technology with great development prospects [2,24].

The PEMWE mainly uses perfluorinated sulfonic acid solid polymer as an electrolyte and Ir, Ru, or Pt-based precious metals as catalysts [25–27]. Essentially, PEMWE is a reverse device of the PEM fuel cell (PEMFC) [28,29]. The PEMWE uses an external power supply to make water electrolysis to generate hydrogen and oxygen. During the PEMWE, as shown in Figure 1, pure water is sent to the anode through the anode bipolar plate with the water pump, then penetrates into the porous diffusion layer, and reaches the catalytic layer. Oxygen evolution reaction (OER) will occur at the anode to produce oxygen ( $O_2$ ), protons ( $H^+$ ), and electrons ( $e^-$ ). These protons diffuse to the cathode side through the PEM, and the electrons leave the anode through the external power circuit [30–32]. After the protons reach the cathode, the electrons transported by the cathode catalyst layer and the external power supply will recombine with them to create a hydrogen evolution reaction (HER) [21]. Figure 1 shows its working principle. The specific equation is as follows:



In PEMWE, the anode is the main source of the entire overvoltage, and the anode electrocatalyst has a very important influence on the entire water electrolysis reaction [33–35]. At present, the preparation of highly active and stable oxygen evolution electrocatalysts has been the key problem in PEMWE, and a lot of research has been carried out around the world [36,37]. At the same time, due to the high potential, strong oxidation, and acidic solution environment of the anode of PEMWE, general carbon materials and metal materials are very easily corroded and dissolved in PEMWE, which leads to the destruction of the bipolar plate structure [38]. Therefore, titanium with high stability and conductivity has become one of the most promising metal materials for preparing the diffusion layer in PEMWE [39,40]. However, the high cost of titanium is still the limiting condition for its large-scale application.

The bottleneck of PEMWE lies in its cost and service life [41]. The research on reducing the cost of PEMWE focuses on the core components such as the catalyst, membrane electrode, gas diffusion layer, and bipolar plates (BPs). Among them, BP, also known as a flow field plate, is one of the key materials of PEMWE cell, accounting for about 48% of the total cost of the cell [42–44]. Reducing the cost of BPs is of importance for the application of the PEMWE. The BP is engraved with flow channels (such as parallel flow field, cross

finger flow field, bionic flow field, etc.). In the process of water electrolysis, the bipolar plate plays the role of conducting electrons, delivering and distributing reactant water to the anode, and collecting and outputting products  $H_2$  and  $O_2$ . As the core component of PEMWE, it is also of great significance to the output power, service life, and cost control of PEMWE cell [1]. Therefore, in addition to the optimization of plate flow channel design, the research on BPs also needs to pay attention to BP materials and protective coating as shown in Figure 2. BPs need not only excellent conductivity but also good corrosion resistance and a process convenient for mass production to adapt to the harsh environment, e.g., high potential and acidic environment in PEMWE cell [45,46].

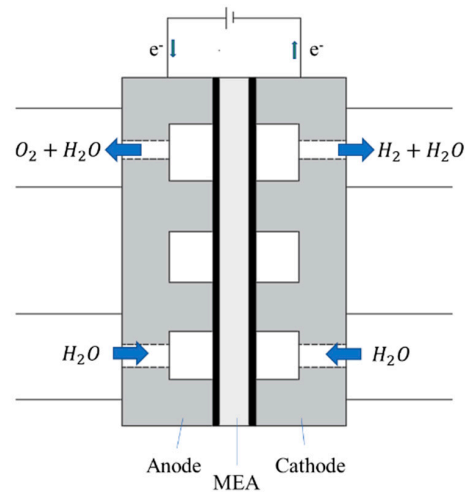


**Figure 1.** Schematic diagram of PEMWE working principle.

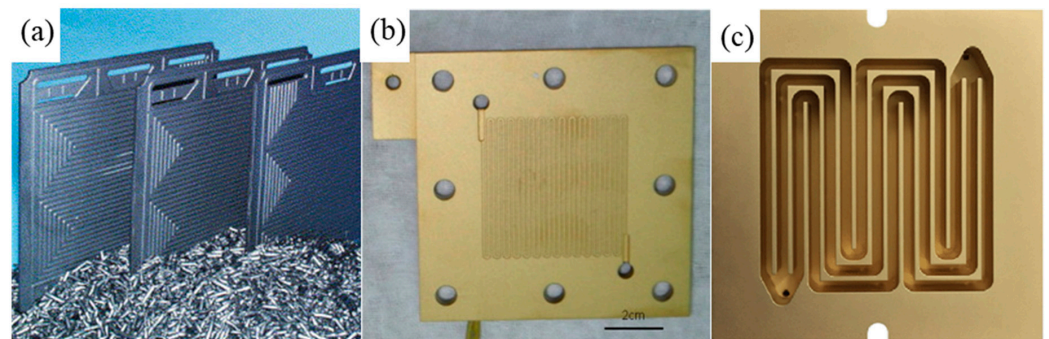


**Figure 2.** The photos of bipolar plate with (a) polymer coating [47], (b) TiN coating [48] and (c) gold coating [49].

Metallic materials are very suitable for BP because of their good plasticity, high conductivity, and high strength [50,51]. Particularly, stainless steel and titanium BPs feature the advantages of high corrosion resistance, high strength, high thermal conductivity, low permeability, and low resistivity. The titanium BPs exhibit good corrosion resistance in the high potential and acidic environment of PEMWE, and the corrosion products of titanium BP are far less toxic to the proton exchange membrane and catalyst than other metals [52,53]. However, during PEMWE operation, an acidic environment and high potential will cause a dense oxide film on the surface of a titanium BP, increasing the interface contact resistance with the collector, thus increasing the ohmic loss, and reducing the output power of the stack [54]. Moreover, hydrogen embrittlement of titanium also exists during the HER (cathode), which is unacceptable for long-term operation. In long-term operation, the titanium plate will absorb more than 1000 ppm hydrogen during 500 h of operation [55,56]. Hydrogen embrittlement can damage the mechanical properties of titanium, such as loss of ductility and tensile strength [57,58]. The modification of the

titanium BPs with protective coatings can greatly reduce the corrosion rate. The commonly investigated measure of a bipolar plate is to prepare a layer of highly conductive and corrosion-resistant coating on the surface. At present, the surface modification of BP coating mainly includes: (1) precious metal coating, such as Au, Pt, etc., prepared on the substrate surface [59]; (2) metal nitrides/carbide coating [46,60]; and (3) conductive polymer coatings [61].

The Au, Pt, and other precious metal coatings modified BPs (Figure 2) have excellent performance and can meet the requirements of PEMWE [59,62]. There is quite a bit of research on mixing these precious metals with other non-noble metal nanomaterials to form a composite coating in order to reduce the usage of precious metals. It is true that both improved corrosion resistance as well as low interfacial contact resistance have been achieved. However, the high cost still limits its commercial development. While for the metal nitrides/carbide coating, the coating process is mainly carried out via *chemical vapor deposition* (CVD) [63,64], physical vapor deposition (PVD) [65,66], and other technologies, which have high equipment requirements or thermal treatment under high temperatures and special atmosphere oven, and they are not suitable for large-scale commercial production.

Generally, the research on the surface modification of metallic BPs for PEMFC is commonly used for reference in the PEMWE application, and there is not much research in the area of PEMWE. However, there is an urgent demand for “solving the corrosion resistance problem of metallic BPs without affecting the contact resistance” which is of great significance to the commercial applications of PEMWE and has gradually become a research hotspot. Herein, there exist several surface modifications of metallic BPs based on silane treatment, conductive polymers, e.g., polyaniline [67] and PPy [68–70], as well as some nanoparticle-promoted polymer hybrid coatings that have both good electrical conductivity and good corrosion resistance and have been investigated for PEMWE. The application of conductive polymers and some nanoparticle-promoted polymer hybrid coatings has a bright future, as the preparation process of polymer coatings is simple, inexpensive, and suitable for large-scale production (Table 1) [71,72]. In this review, both the pretreatment of the metal surface with silane treatment technology and the mechanism and application of the conductive polymers and polymer-based hybrid coatings to prevent the oxidization and the hydrogen embrittlement of the metallic surface are summarized for the first time. It is believed that this review could enrich the knowledge of the large-scale preparation process and applications of polymer-based coatings for PEMWE.

**Table 1.** Comparison of different coatings.

Bipolar Plate Materials	Polymer Coatings	Nitride Coatings	Precious Metal Coatings
Coating methods	silica sol–gel, Nanocasting	Thermal nitriding process	Pulse current electrodeposition, PVD
Materials	Conductive polymers	Nitrides	Rare and precious metals
Chemical stability	good	good	good
Electrical conductivity	fair	fair	good
Thermal conductivity	good	fair	good
Corrosion resistance	good	good	good
Scratch resistance	good	fair	fair
Pitting corrosion resistance	good	fair	fair
Process complexity	easy	complex	fair
Cost	low	low	high

## 2. Silane Treatment Technology

As a new technology, silane treatment technology can significantly improve the corrosion resistance of metal by preparing a layer of silane coating on the metal surface [73,74]. The dense silane layer not only undertakes the charge transfer from the metal surface to the electrolyte solution interface as a conductive layer but also restricts the direct contact between metal and electrolyte solution as an effective isolation layer, which is considered

to be the reason why the silane layer can effectively improve the corrosion resistance of metal [75,76]. In addition, organic silane coating can be used as a “bridge” for the close connection between metal and other polymer coatings, greatly improving the adhesion between the organic coating and the metal. Silane treatment has the advantages of simple operation, strong adhesion, and environmental safety. Generally, the silane coating has a wide application prospect, and it is affected by the polarity of functional groups of silane itself. Silane coupling agents are generally divided into hydrophobic and hydrophilic. Silanes with non-polar functional groups are hydrophobic and need to use a cosolvent to make them soluble in water for hydrolysis. The structure of silane is generally  $Y-R-SiX_3$  or  $R'-(CH_2)_n-Si(OR)_3$  where R is an aliphatic carbon chain, R' (or Y) is a group that can react with organic compounds (such as epoxy group, amino group, etc.) to improve the compatibility and reactivity of polymer and silane, and OR (or X) is a hydrolytic group (such as acetoxy, alkoxy, etc.), which can bond some metals,  $SiO_2$ , etc. Because of these two functions, silane molecules can connect organic materials and inorganic materials to form an “organic silane chain inorganic” intermediate layer with a certain network structure. Edzatty et al. [77] pointed out that hydroxysilane with a carbon functional group can be used for metal surface treatment. If the silane coupling agent does not have an organic group, it can generally be used to prepare a single protective film. For example, compounds with epoxy silane that can match the coating generally have specific carbon functional groups, which can improve the adhesion between the substrate and the organic coating [78].

There are many causes for silane molecules to adsorb and form films on the surface of metal substrates. At present, most people believe that the chemical bond theory proposed is the closest to the actual situation [79,80]. Figure 3 shows the theoretical model of the silane chemical bond, which summarizes the action process of silane on the substrate surface in three steps:

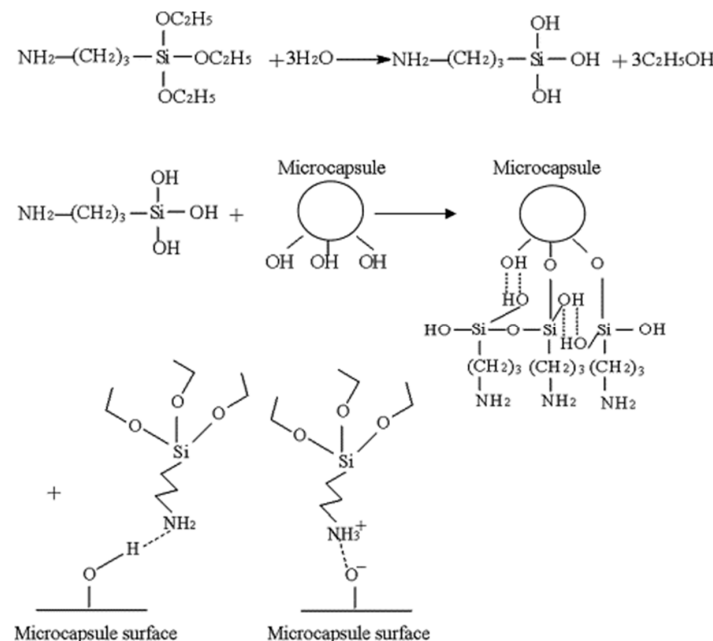
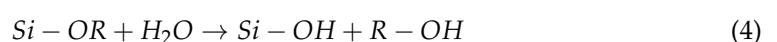
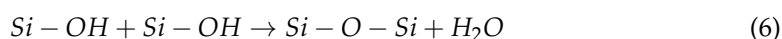
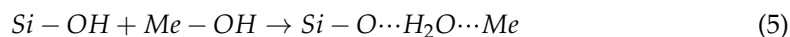


**Figure 3.** Theoretical model of chemical bonding of silane coupling agent [78].

(1) Activation of silane molecules. Hydrolysis reaction will occur during the preparation of silane. Under the action of water molecules, the Si-X group will hydrolyze to generate Si-OH, as shown in formula (4). With the gradual hydrolysis of  $(Si-OR)_n$ , a large amount of Si-OH will be generated in the solution, which will activate the silane molecules for further reaction.



(2) Adsorption and condensation of silane molecules. After the metal substrate is put into the silane hydrolysate, the activated Si-OH and hydroxylated substrate surface (i.e., Me-OH group) are rapidly combined in the form of hydrogen bond, so as to adsorb on the metal surface, as shown in formula (5). At the same time, there are still a large number of active Si-OH groups in the solution [81,82]. Adjacent Si-OH is prone to intermolecular dehydration and condensation reaction, forming an outer silane membrane with a Si-O-Si interpenetrating network structure, as shown in formula (6).



(3) Silane molecules are solidified into films. After adsorption, silane molecules are solidified on the surface of the substrate. In this process, due to the instability of the hydrogen bond,  $Si - O \cdots H_2O \cdots Me$  groups lose one molecular water and form stable  $Si-O-Me$  covalent bonds, as shown in formula (7). The curing and film forming need to be heated at a certain temperature. Different silane curing processes need different temperatures. Generally, the curing temperature should be greater than 90 °C. During the curing process, a dehydration reaction will occur between hydrogen bonds, forming  $Si-O-Me$  bonds at the interface where the surface metal participates in bonding, which can significantly improve the bonding strength between the metal matrix and silane. At the same time, the remaining silanol hydroxyl groups adsorbed on the surface of the matrix that do not participate in bonding at the interface will dehydrate and condense with each other to form  $Si-O-Si$  bonds, thus forming a layer of cross-linked mesh three-dimensional silane film on the metal surface. Generally, one end of the silane coupling agent is hydrolyzed with three silanol hydroxyl groups, but the energy required for bonding with the metal substrate surface is different. When one silanol hydroxyl group is bonded, the other two will no longer bond, or dehydrate and condense with the silanol hydroxyl groups in adjacent molecules, or finally exist in the silane film in a free state at one end.



The complete impregnation method and electrodeposition method are the main methods for preparing silane membranes on metal surfaces. Under the action of hydrogen bonding, the silane solution will quickly adsorb to the metal surface after contact with the metal, compared to mature chromate passivation that requires a longer period of dipping, and silanes take much less time to complete adsorption on metal surfaces.

Generally, the surface modification of the metal surface with silane has the following advantages: simple process, non-toxic, non-polluting, a wide range of applications, low cost, and the anticorrosion effect is better than the traditional phosphating, and passivation process. The silane-treated metal surface can also enhance the adhesion between the metal matrix and organic coating.

### 3. Conductive Polymer Based Coating

#### 3.1. Polyaniline (PANI)

PANI is one of the earliest found conjugated conductive polymers, and its conductivity is between 5 and 10 S cm<sup>-1</sup>. Polyaniline is a typical organic conductive polymer, and although the  $\pi$  electrons in its structure have the ability to delocalize, it is not a free electron. The conjugated structure in the molecule increases the  $\pi$  electron system; the electron delocalization is enhanced. When the conjugated structure reaches a large enough scale, the compound can provide free electrons, so as to be able to conduct electricity.

Many studies on the mechanism and applications of polyaniline in metal corrosion prevention show that the corrosion prevention mechanism of polyaniline on metal mainly has several points (Figure 4): (1) Wessling's [83] research on metal passivation theory found that doped polyaniline can catalyze itself and form a passivation film on the metal surface

after oxidation by first reducing. In addition, polyaniline has a self-repairing effect. When the passivation film is damaged, polyaniline can repair the passive film and maintain its stable existence for a long time. (2) Shielding effect: it was found by electrochemical impedance spectroscopy (EIS) that when the thickness of electrochemical polymerized polyaniline coating was greater than 1  $\mu\text{m}$ , the polyaniline coating can completely separate the metal from the corrosion medium, significantly delaying the metal corrosion, which is the physical shielding effect of the polyaniline coating [84]. (3) Electric field protection of polyaniline will generate a special electric field at the metal interface. During corrosion, the direction of electron transmission is opposite to that of the electric field. The electric field force becomes an important factor preventing the movement of electrons from the metal to the oxidant. At this time, the metal surface is protected by the electric field [85]. In recent years, polyaniline has obtained more and more applications in the field of hydrogen energy due to its protective effect on metals. Jiang et al. [86] deposited a polyaniline layer of 2.5  $\mu\text{m}$  on the surface of 304 stainless steel, showing stable structural characteristics and good corrosion resistance. The adhesion characteristics of the polyaniline coating on the 304 stainless steel did not change significantly within 648 h, and the polarization current density was stable at  $0.059 \mu\text{A cm}^{-2}$ , which is significantly better than the original 304 stainless steel, revealing the great potential of polyaniline in the field of metal BP coating.

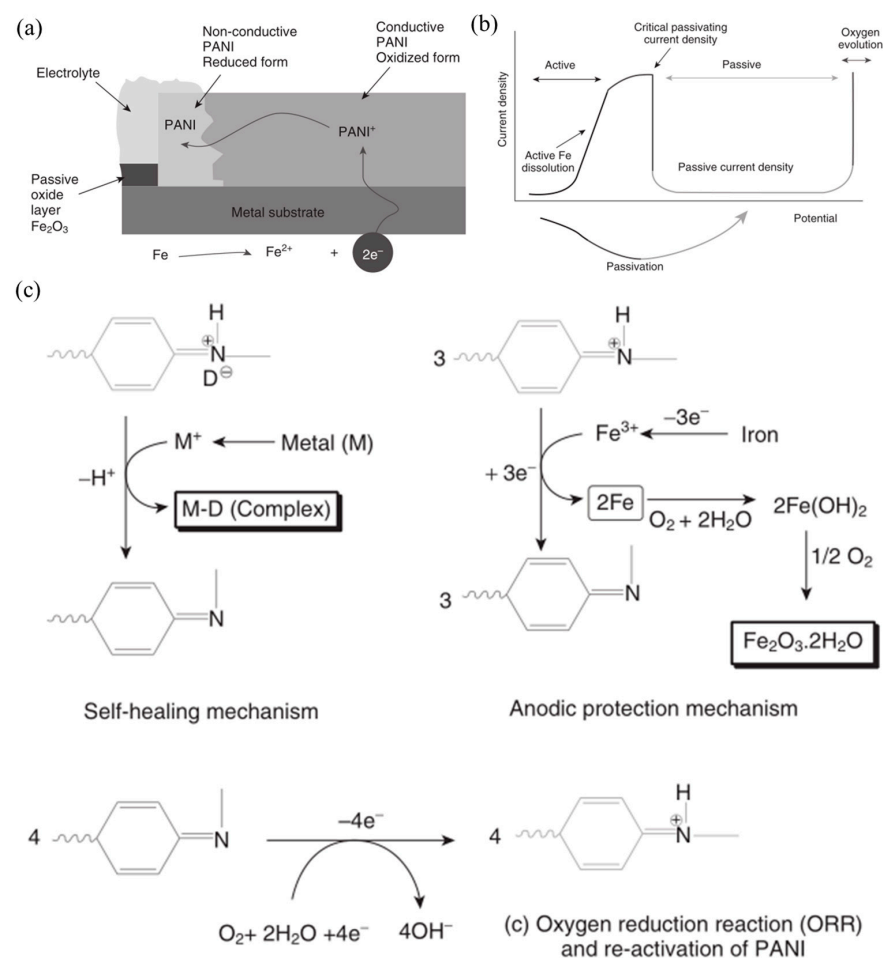


**Figure 4.** (a) The concept of ennobling mechanism using PANI. (b) Corrosion protection of iron electrode coated with conductive polymer. Two mechanisms can be identified: (1) barrier protection of the PANI coating suppresses the active metal dissolution, and (2) ennobling effect due to the redox activity of the PANI which shifts the potential into a passive domain at higher potential values. (c) Schematic illustration for the chemical reactions of PANI for corrosion protection of iron through different mechanisms [87].

### 3.2. Polypyrrole (PPy)

PPy is a kind of heterocyclic conjugated conductive polymer with pyrrole as a monomer and is made into a conductive film by electrochemical oxidation polymerization or synthesized by the chemical polymerization method [68,88]. It is a conductive polymer with good stability and easy electrochemical polymerization into a film, and its conductivity can reach  $10^2$ – $10^3$  S cm<sup>-1</sup>. The conduction mechanism is: the PPy structure has a conjugated structure composed of carbon–carbon single bonds and carbon–carbon double bonds arranged alternately [89,90]. The double bonds are composed of  $\sigma$  electrons and  $\pi$  electrons, and  $\sigma$  electrons are fixed and cannot move freely, forming covalent bonds between carbon atoms [91]. The 2  $\pi$  electrons in a conjugated double bond are not fixed to a certain carbon atom, they can transpose from one carbon atom to another: that is, they have a tendency to extend throughout the molecular chain [92].

Tan et al. [93] (Figure 5) successfully prepared Ti<sub>4</sub>O<sub>7</sub> nanoparticles using titanium powder as a reducing agent, and then prepared a dense Ti<sub>4</sub>O<sub>7</sub> nanoparticles doped polypyrrole (PPy) composite coating on the 316 L surface using constant current deposition technology. Conductive Ti<sub>4</sub>O<sub>7</sub> nanoparticles were modified with methyl sulfonic acid. Ti<sub>4</sub>O<sub>7</sub> nanoparticles were combined with sulfur-doped acid and the PPy chain through electrostatic action as well. In the cathode environment of PEMFC, the composite coating maintained high chemical stability. At the same time, the addition of Ti<sub>4</sub>O<sub>7</sub> nanoparticles also improved the conductivity and hydrophobicity of the PPy coating. In further study, the PPy-Ti<sub>4</sub>O<sub>7</sub> coating showed amazing stability, and the impedance was basically maintained between 5.78 and 6.80  $\Omega$  cm<sup>2</sup> within 50 h in the simulated environment at 70 °C. Akula et al. [94] applied conductive polymer (2-amino-5-mercapto-1,3,4-thiadiazole)/polypyrrole (PAMT/PPy) single-layer and double-layer conductive composite coatings on 316 L stainless steel using the cyclic voltammetry and galvanostatic method. The polarization measurements of the coating by cyclic voltammetry (CV) showed that compared with PPy on the PAMT double-layer coating, the PAMT on the PPy double-layer coating has lower corrosion current density. It was also found the PAMT on PPy double-layer coating showed better chemical stability than the PAMT/PPy single layer and PPy on PAMT double layers, and the corrosion potential was about 250 mV. Under the simulated PEMFC conditions, the performance of the coating was studied in the anode (0.1 V and H<sub>2</sub> purging) and cathode (0.6 V, oxygen purging) environments for 12 h to evaluate the stability of the coating. Under these conditions, all coatings except for the PPy coating were stable in both environments. Although the cost of these conductive polymer coatings is much lower than that of precious metal coatings, in the PEMWE working environment, high temperature will cause partial decomposition, thus losing the protection of the substrate, and the coating may fall off after a long time of operation [87].

Josep et al. [61] found that with the increase of cycles, the coating became thicker, and the adhesion decreased. The pinholes in the polyaniline coating increased with the increase of deposition cycles, while the pinholes in PPy had little or no increase with the increase of deposition cycles. In polyaniline and PPy coatings, the corrosion effect was the best after three deposition cycles. Under the same compaction pressure, the contact resistance of a polymer-coated plate deposited by three cycles was very close to that of the graphite plate. The conductivity of these polymer coatings is expected to improve under the acidic conditions of actual fuel cells.

Compared with PPy, PANI could be a potential conductive polymer due to its excellent performance and relatively simple preparation method. However, the electrical conductivity still requires further improvement and the serious peeling off of the coating during long-term operation also needs to be solved. Currently, conductive polymer combined with graphene, metals, and their compounds in the form of nanoparticle-promoted polymer hybrid coatings could be a good choice to obtain higher corrosion resistance, durability, and conductivity and to extend the service life of PEMWE.

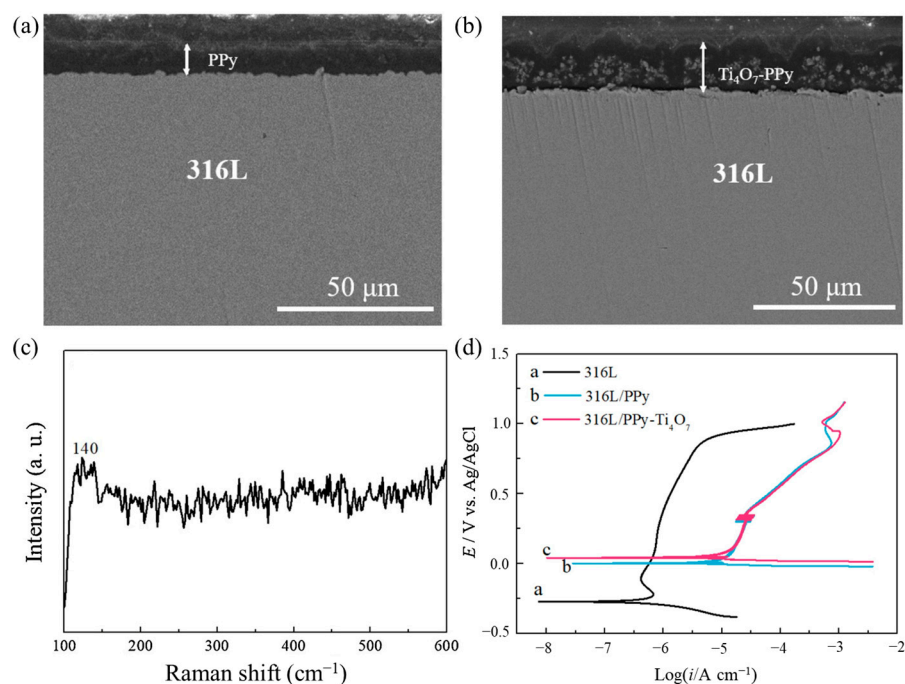


**Figure 5.** The cross-sectional morphologies of (a) PPy and (b) PPy-Ti<sub>4</sub>O<sub>7</sub> nanoparticles, (c) the Raman spectra curves of PPy-Ti<sub>4</sub>O<sub>7</sub> nanoparticles coating with 10% PPy, and (d) the potentiodynamic polarization curves of 316 L, 316 L/PPy, and 316 L/PPy-Ti<sub>4</sub>O<sub>7</sub> nanoparticles samples immersed in 0.1 M H<sub>2</sub>SO<sub>4</sub>/2 ppm HF solution at 25 °C for 1 h [93].

#### 4. Nanoparticles-Promoted Polymer Hybrid Coatings

##### 4.1. Epoxy Resin (EP)-Based Hybrid Coatings

As a low molecular weight prepolymer with one or more epoxy groups, epoxy resin is mainly obtained by using different types of curing agents to participate in the curing reaction. Its performance is mainly determined by the type of epoxy resin and the combination mode of the curing agent used. Epoxy resin is widely used in fiber-reinforced materials, general adhesives, packaging materials, high-performance anticorrosion coatings, and other fields due to its high hardness, good chemical and mechanical resistance, high adhesion to many substrates, and good thermal performance [95,96]. Luo et al. [97] (Figure 6) investigated the hybrid coating with the graphene nanolayers dispersed in epoxy resin. Its anticorrosion performance was tested by electrochemical tests and salt spray tests. The results showed that only 0.5% graphene content can achieve the best anticorrosion performance, and its protective effect on Q235 steel sheet reached 99.7%. Abdullah et al. [98] used graphene oxide (GO) to modify epoxy resin to prepare GO/EP composites. They found that the tensile strength of the composites first increased and then decreased with the increase of GO volume fraction. When the GO volume fraction was 1.5%, the Lakun strength reached the maximum value of 13 MPa. When the GO volume fraction was >1.5%, due to the large specific surface area of GO, its own agglomeration was strengthened, the stress distribution was uneven, and the tensile strength decreased. Argüelles et al. [99] found that when thermal reduced GO (TRGO) was added to the one-component and two-component EP matrix, the reinforcing ability of TRGO to the one-component EP was lower than that of the two-component EP, and the TRGO with a mass fraction of 1% increased the tensile strength of the two-component composites.

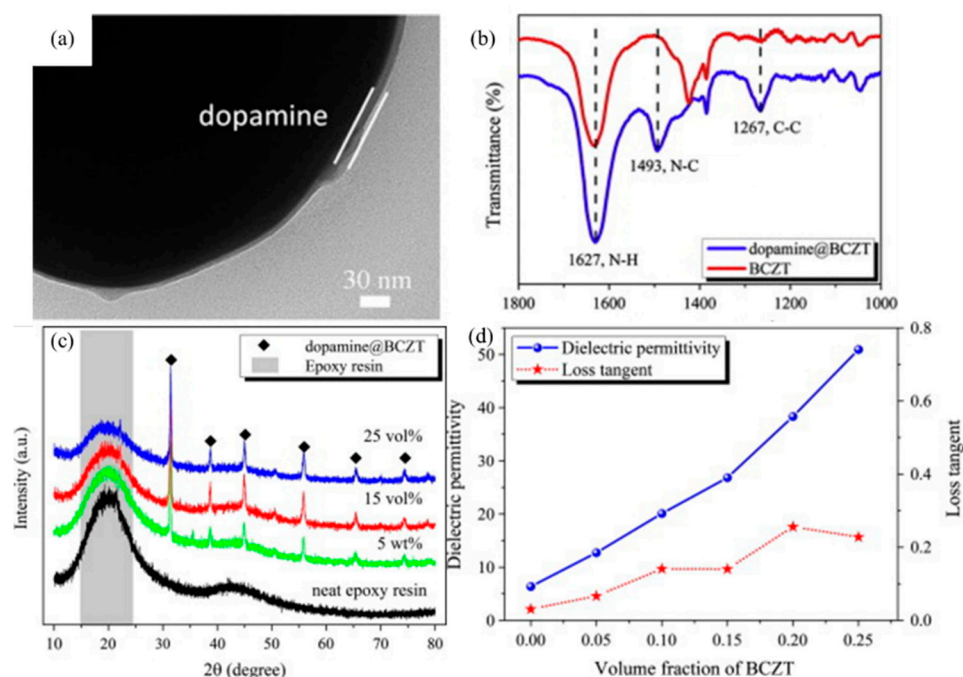


**Figure 6.** (a) The TEM image of dopamine@BCZT powders, the coating layer is about 15 nm; (b) FTIR spectra of ceramic powders before and after dopamine modification. (c) The XRD patterns of ceramic/epoxy resin composites with different volume fractions of dopamine@BCZT powders. (d) The dielectric constant and dielectric loss tangent of dopamine@BCZT/epoxy resin composites with various concentrations of dopamine@BCZT powders at 1000 Hz and room temperature [100].

#### 4.2. Polyimide (PI) Based Hybrid Coatings

Polyimide (PI) is a kind of polymer with an imide ring in the main chain, among which the polymer with phthalimide structure is more important [101,102]. According to the structural unit of the molecule, they can generally be divided into aliphatic PIs and aromatic PIs. Because of the poor practicability of aliphatic PIs, polymers with aromatic PIs are particularly important. PI, as a kind of special engineering plastic with excellent performance, is also one of the polymer materials with the highest heat resistance rating so far. Because of its excellent performance, it is widely used in high-tech fields such as microelectronics, separation membranes, aerospace, and so on. PI has strong high-temperature resistance, its glass transition temperature is generally above 200 °C, and the most important feature of all aromatic PI is its good heat resistance, its thermal decomposition temperature can often reach 500 °C, and brittle behavior will not occur at ultra-low temperatures. In addition, it has very high mechanical strength and a low thermal expansion coefficient, which means that PI film can maintain good physical protection performance in a hot and humid environment. Furthermore, PI has excellent dielectric properties, and its dielectric constant is about 3.4. When fluorine is introduced into PI, its dielectric constant can be reduced to ca. 2.5. This makes it widely used in the electrical insulation industry, as the outer coating of insulated wire or direct coating. Due to the self-lubricating property of PI, it can resist aging and electrical breakdown.

Due to the excellent properties of PI, it has a great prospect in the application of high corrosion resistance coatings, especially in corrosion protection under harsh chemical media and mechanical damage conditions. Jia et al. [103,104] (Figure 7) prepared TRGO/PI nanocomposite corrosion-resistant coatings with different mass fractions by adding high-temperature thermally reduced graphene oxide (TRGO) as a two-dimensional nanofiller to the PI polymer matrix and evaluated the electrochemical corrosion behavior of the coating in simulated seawater (3.5 wt% NaCl solution) using alternating current impedance spectroscopy and potentiodynamic polarization curves. The results showed that the addition of TRGO could significantly improve the resistance and corrosion protection efficiency of

the coating. When the TRGO content was 0.3 wt%, the corrosion resistance of the coating was best enhanced, and the maximum coating resistance was  $1.3176 \times 10^6 \Omega$ , the highest corrosion protection efficiency reached 99.65%, and its corrosion protection gain was related to the excellent physical and chemical properties of PI and the physical barrier performance of TRGO.

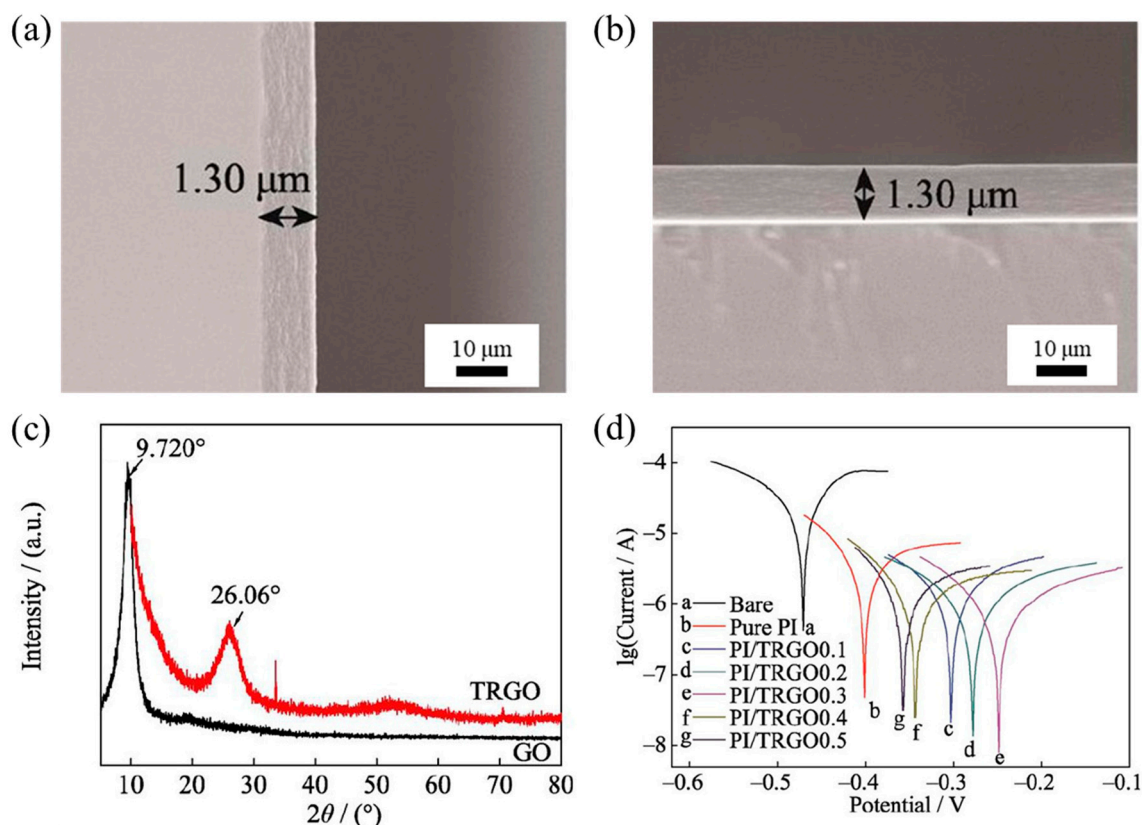


**Figure 7.** Photographs of the fractured surfaces of (a) the neat PI and (b) the TRGO0.1/PI coatings, (c) XRD patterns of GO and TRGO. (d) Tafel plots of the bare steel, pure PI, and TRGO/PI coatings [104].

#### 4.3. Other Polymer-Based Hybrid Coatings

Liu et al. [105] electrophoretically deposited a layer of highly conductive and corrosion-resistant graphene on metal BPs. In order to avoid the oxidation of metal substrate during the electrophoretic deposition (EPD), p-phenylenediamine (PPD) was first grafted onto GO to obtain modified GO. Then, under a constant voltage, magnesium oxide dispersed in ethanol was coated on a titanium plate through cathodic EPD. Next, the deposited magnesium oxide was reduced with  $H_2$  at  $400^\circ C$  to obtain a titanium plate coated with reduced magnesium oxide (RMGO@Ti). Under the simulated environment of PEMFC, the RMGO@Ti revealed a corrosion current of less than  $10^{-6} A cm^{-2}$ , about two orders of magnitude lower than that of the pure titanium. In addition, the ICR was studied for the RMGO@Ti, which was as low as  $4 m\Omega cm^2$ , about one-thirtieth of the bare titanium. Lee et al. [106] used EPD technology to coat a layer of titanium nitride (TiN) nanoparticles on the stainless steel surface as the BP of PEMFC. The charging additive was polydimethyl-diallylammonium chloride (PDADMAC), and titanium nitride powder was uniformly deposited on stainless steel by EPD. The effects of time, voltage, pH value, and different charging agents on the uniformity and kinetics of TiN nanoparticles were studied. The results showed that the deposition rate and surface morphology of PDADMAC with different chain lengths were different.

Liu et al. [107] prepared a hydrophilic corrosion-resistant polydopamine (PDA) composite protective coating. A layer of PDA film was prepared on the surface of titanium by solution oxidation. The Au nanoparticles mounted on PDA using an in situ reduction method improved the conductivity and corrosion resistance; however, it was found that the Au-PDA coating was not particularly suitable for modifying titanium porous diffusion layers in PEMWE systems. The modification of the coating reduced the polarization current density of the diffusion layer to  $0.001 \mu\text{A cm}^{-2}$ , which is an order of magnitude reduction compared to the pure titanium.

Nanoparticle-reinforced polymer hybrid coating has the characteristics of easy processing, good corrosion resistance, and excellent mechanical properties. The mechanical properties of polymer coatings are also affected by the feature of nanosized conductive particles, such as the conductive materials, addition amount, dispersion of nanoparticles, and other factors, which need to be carefully controlled to balance the conductive and mechanical properties of the coatings. As for the selection of different kinds of polymers, compared with the PI-based thermoplastic coating, the epoxy resin coating is a thermosetting polymer, which has the advantages of high conductivity and high bending strength, but the disadvantage is that it has a long processing cycle and is not conducive to large-scale production [108,109].

## 5. Conclusions and Perspectives

Among the various water electrolysis hydrogen production technologies, PEMWE has the advantages of high current density, high purity of hydrogen production, and fast response speed, which has attracted wide attention from the scientific community and industry. Electrolysis efficiency, cost, and life are important indicators of PEMWE. As a supporting part and current collector of the PEMWE cell, the BPs require high corrosion resistance and low interfacial resistance. The industries generally believe that metallic BPs are a potential choice for PEMWE in the future, which can be manufactured through an embossing process with a low cost, thin thickness, and high-volume specific power and specific energy density. However, the corrosion and passivation of the metallic surface during the operation of PEMWE could result in high ICR during the long-term operation and, thus, increase the ohmic loss, and reduce the output power of the stack. This puts forward the urgent demand of “solving the corrosion resistance problem of metallic BPs without affecting the contact resistance”. Currently, metallic BPs with protective coatings, such as precious metals, nitrides, carbides, etc., are effective ways. While the disadvantage of the precious metal coating is high cost, it has high conductivity and remarkable corrosion resistance. While the titanium nitrides/carbide coatings, which have high equipment requirements or thermal treatment under high temperatures and special atmosphere oven, are not suitable for large-scale commercial production.

At present, the surface modification of metallic BPs based on conductive polymers, such as silane treatment, PANI, PPy, and polymer mixed layers promoted by some nanoparticles, have good corrosion resistance, excellent conductivity, and low production cost, which is one of the development trends. The aim of this review is to summarize and discuss the protective mechanisms, preparation processes, and applications of the above-mentioned polymer-based coatings of BPs for PEMWE in depth. (1) As for the silane treatment, the dense silane layer can not only effectively enhance the corrosion resistance but also improve the adhesion between the substrate and the conductive polymers. (2) As for the conductive polymeric coatings, the poor electrical conductivity of the polymer and serious peeling off during long-term operation greatly limit the application according to the literature. (3) While for the nanoparticle-promoted polymer hybrid coatings, the composition, dispersion of nanoparticles, microstructure, etc., can be controlled to balance the conductivity and mechanical properties. Especially, nanoparticle-promoted polymer hybrid coatings composed of polymers and conductive noble metals or nitrides/carbides, which have the advantages of a simple preparation process, low cost, and large-scale production, are of

great significance to the commercial applications of PEMWE and have gradually become a research hotspot.

**Author Contributions:** Conceptualization, G.L. and F.H.; validation, G.L. and F.H.; formal analysis, G.L. and F.H.; investigation, G.L. and F.H.; resources, G.L.; data curation, G.L. writing—original draft preparation, G.L. and B.F.; writing—review and editing, G.L., B.F., and X.W.; visualization, G.L. and B.F.; supervision, G.L.; project administration, G.L.; funding acquisition, G.L. All authors have read and agreed to the published version of the manuscript.

**Funding:** This research was funded by the National Key Research and Development plan of China (Grant No. 2018YFB1502403) and the Communication Program for Young Scientist in USTB (Grant No. QNXM20220015).

**Institutional Review Board Statement:** Not applicable.

**Informed Consent Statement:** Not applicable.

**Data Availability Statement:** Data will be available upon request from the corresponding authors.

**Conflicts of Interest:** The authors declare no conflict of interest.

## Abbreviations

Abbreviation	Definition
PEMWE	Proton exchange membrane water electrolysis
BPs	Bipolar plates
PANI	Polyaniline
PPy	Polypyrrole
ICR	Interface contact resistance
PEMFC	Proton exchange membrane fuel cell
OER	Oxygen evolution reaction
HER	Hydrogen evolution reaction
CVD	Chemical vapor deposition
PVD	Physical vapor deposition
EIS	Electrochemical impedance spectroscopy
CV	Cyclic voltammetry
PAMT	2-amino-5-mercapto-1,3,4-thiadiazole
EP	Epoxy resin
GO	Grapheme oxide
TRGO	thermal reduced grapheme oxide
BCZT	Ba <sub>0.85</sub> Ca <sub>0.15</sub> Zr <sub>0.1</sub> Ti <sub>0.9</sub> O <sub>3</sub>
FTIR	Fourier transform infrared spectroscopy
PI	Polyimide
EPD	Electrophoretic deposition
PPD	P-phenylenediamine
TiN	Titanium nitride
RMGO	Reduced magnesium oxide
PDADMAC	Polydimethyldiallylammonium chloride
Polydopamine	PDA

## References

1. Carmo, M.; Fritz, D.L.; Mergel, J.; Stolten, D. A comprehensive review on PEM water electrolysis. *Int. J. Hydrogen Energy* **2013**, *38*, 4901–4934. [[CrossRef](#)]
2. Vincent, I.; Bessarabov, D. Low cost hydrogen production by anion exchange membrane electrolysis: A review. *Renew. Sustain. Energy Rev.* **2018**, *81*, 1690–1704. [[CrossRef](#)]
3. Bezdek, R.H. The hydrogen economy and jobs of the future. *Renew. Energy Environ. Sustain.* **2020**, *96*, 107. [[CrossRef](#)]
4. Li, C.; Liao, G.; Fang, B. Magnetic-field-promoted photocatalytic overall water-splitting systems. *Chem. Catal.* **2022**, *2*, 238–241. [[CrossRef](#)]
5. Liao, G.; Li, C.; Fang, B. Donor-acceptor organic semiconductor heterojunction nanoparticles for efficient photocatalytic H<sub>2</sub> evolution. *Matter* **2022**, *5*, 1635–1637. [[CrossRef](#)]

6. Liao, G.; Li, C.; Liu, S.Y.; Fang, B.; Yang, H. Z-scheme systems: From fundamental principles to characterization, synthesis, and photocatalytic fuel-conversion applications. *Phys. Rep.* **2022**, *983*, 1–41. [[CrossRef](#)]
7. Liao, G.; Li, C.; Liu, S.Y.; Fang, B.; Yang, H. Emerging frontiers of Z-scheme photocatalytic systems. *Trends Chem.* **2022**, *4*, 111–127. [[CrossRef](#)]
8. Liu, Y.; Xu, G.; Ma, D.; Li, Z.; Yan, Z.; Xu, A.; Zhong, W.; Fang, B. Synergistic effects of g-C<sub>3</sub>N<sub>4</sub> three-dimensional inverse opals and Ag modification toward high-efficiency photocatalytic H<sub>2</sub> evolution. *J. Clean. Prod.* **2021**, *328*, 129745. [[CrossRef](#)]
9. Reilly, K.; Adeli, B.; Fang, B.; Wilkinson, D.P.; Taghipour, F. Advanced titanium dioxide fluidizable nanowire photocatalysts. *RSC Adv.* **2022**, *12*, 4240–4252. [[CrossRef](#)]
10. Xu, G.; Cai, X.; Wang, L.; Zhang, Q.; Fang, B.; Zhong, X.; Yao, J. Thermogravimetric-infrared analysis and performance optimization of co-pyrolysis of oily sludge and rice husks. *Int. J. Hydrogen Energy* **2022**, *47*, 27437–27451. [[CrossRef](#)]
11. Smith, D.W.; Oladoyinbo, F.O.; Mortimore, W.A.; Colquhoun, H.M.; Thomassen, M.S.; Ødegård, A.; Guillet, N.; Mayousse, E.; Klicpera, T.; Hayes, W. A Microblock Ionomer in Proton Exchange Membrane Electrolysis for the Production of High Purity Hydrogen. *Macromolecules* **2013**, *46*, 1504–1511. [[CrossRef](#)]
12. Moschovi, A.M.; Zagoraiou, E.; Polyzou, E.; Yakoumis, I. Recycling of Critical Raw Materials from Hydrogen Chemical Storage Stacks (PEMWE), Membrane Electrode Assemblies (MEA) and Electrocatalysts. *IOP Conf. Ser. Mater. Sci. Eng.* **2021**, *1024*, 012008. [[CrossRef](#)]
13. Gohil, J.M.; Dutta, K. Structures and properties of polymers in ion exchange membranes for hydrogen generation by water electrolysis. *Polym. Adv. Technol.* **2021**, *32*, 4598–4615. [[CrossRef](#)]
14. Liu, G.; Hou, F.; Wang, X.; Fang, B. Stainless Steel-Supported Amorphous Nickel Phosphide/Nickel as an Electrocatalyst for Hydrogen Evolution Reaction. *Nanomaterials* **2022**, *12*, 3328. [[CrossRef](#)] [[PubMed](#)]
15. Liu, G.; Hou, F.; Peng, S.; Wang, X.; Fang, B. Synthesis, Physical Properties and Electrocatalytic Performance of Nickel Phosphides for Hydrogen Evolution Reaction of Water Electrolysis. *Nanomaterials* **2022**, *12*, 2935. [[CrossRef](#)] [[PubMed](#)]
16. Liu, G.; Peng, S.; Hou, F.; Wang, X.; Fang, B. Preparation and Performance Study of the Anodic Catalyst Layer via Doctor Blade Coating for PEM Water Electrolysis. *Membranes* **2023**, *13*, 24. [[CrossRef](#)]
17. Liao, G.; Li, C.; Li, X.; Fang, B. Emerging polymeric carbon nitride Z-scheme systems for photocatalysis. *Cell Rep. Phys. Sci.* **2021**, *2*, 100355. [[CrossRef](#)]
18. Teuku, H.; Alshami, I.; Goh, J.; Masdar, M.S.; Loh, K.S. Review on bipolar plates for low-temperature polymer electrolyte membrane water electrolyzer. *Int. J. Energy Res.* **2021**, *45*, 20583–20600. [[CrossRef](#)]
19. Khatib, F.N.; Wilberforce, T.; Ijaodola, O.; Ogungbemi, E.; El-Hassan, Z.; Durrant, A.; Thompson, J.; Olabi, A.G. Material degradation of components in polymer electrolyte membrane (PEM) electrolytic cell and mitigation mechanisms: A review. *Renew. Sustain. Energy Rev.* **2019**, *111*, 1–14. [[CrossRef](#)]
20. Liu, G.; Hou, F.; Wang, X.; Fang, B. Ir-IrO<sub>2</sub> with heterogeneous interfaces and oxygen vacancies-rich surfaces for highly efficient oxygen evolution reaction. *Appl. Surf. Sci.* **2023**, *615*, 156333. [[CrossRef](#)]
21. Liu, G.; Hou, F.; Wang, X.; Fang, B. Robust Porous TiN Layer for Improved Oxygen Evolution Reaction Performance. *Materials* **2022**, *15*, 7602. [[CrossRef](#)] [[PubMed](#)]
22. Hong, Z.; Wei, Z.; Han, X. Optimization scheduling control strategy of wind-hydrogen system considering hydrogen production efficiency. *J. Energy Storage* **2022**, *47*, 103609. [[CrossRef](#)]
23. Hu, S.; Feng, C.; Wang, S.; Liu, J.; Wu, H.; Zhang, L.; Zhang, J. Ni<sub>3</sub>N/NF as Bifunctional Catalysts for Both Hydrogen Generation and Urea Decomposition. *ACS Appl. Mater. Interfaces* **2019**, *11*, 13168–13175. [[CrossRef](#)] [[PubMed](#)]
24. Feng, Q.; Liu, G.; Wei, B.; Zhang, Z.; Li, H.; Wang, H. A review of proton exchange membrane water electrolysis on degradation mechanisms and mitigation strategies. *J. Power Sources* **2017**, *366*, 33–55. [[CrossRef](#)]
25. Song, J.; Wei, C.; Huang, Z.F.; Liu, C.; Zeng, L.; Wang, X.; Xu, Z.J. A review on fundamentals for designing oxygen evolution electrocatalysts. *Chem. Soc. Rev.* **2020**, *49*, 2196–2214. [[CrossRef](#)]
26. Štrbac, S.; Smiljanić, M.; Wakelin, T.; Potočnik, J.; Rakočević, Z. Hydrogen evolution reaction on bimetallic Ir/Pt(poly) electrodes in alkaline solution. *Electrochim. Acta* **2019**, *306*, 18–27. [[CrossRef](#)]
27. Lu, L.; Zheng, H.; Li, Y.; Zhou, Y.; Fang, B. Ligand-free synthesis of noble metal nanocatalysts for electrocatalysis. *Chem. Eng. J.* **2023**, *451*, 138668. [[CrossRef](#)]
28. Jiménez-Morales, I.; Cavaliere, S.; Dupont, M.; Jones, D.; Rozière, J. On the stability of antimony doped tin oxide supports in proton exchange membrane fuel cell and water electrolyzers. *Sustain. Energy Fuels* **2019**, *3*, 1526–1535. [[CrossRef](#)]
29. Liu, G.; Hou, F.; Peng, S.; Wang, X.; Fang, B. Process and challenges of stainless steel based bipolar plates for proton exchange membrane fuel cells. *Int. J. Miner. Metall. Mater.* **2022**, *29*, 1099–1119. [[CrossRef](#)]
30. Alaswad, A.; Palumbo, A.; Dassisi, M.; Olabi, A.G. Fuel Cell Technologies, Applications, and State of the Art. A Reference Guide. In *Reference Module in Materials Science and Materials Engineering*; Elsevier: Amsterdam, The Netherlands, 2015. [[CrossRef](#)]
31. Das, P.K.; Li, X.; Liu, Z.S. Analytical approach to polymer electrolyte membrane fuel cell performance and optimization. *J. Electroanal. Chem.* **2007**, *604*, 72–90. [[CrossRef](#)]
32. Khan, M.A.; Zhao, H.; Zou, W.; Chen, Z.; Cao, W.; Fang, J.; Xu, J.; Zhang, L.; Zhang, J. Recent Progresses in Electrocatalysts for Water Electrolysis. *Electrochem. Energy Rev.* **2018**, *1*, 483–530. [[CrossRef](#)]
33. Shirvanian, P.; van Berkel, F. Novel components in Proton Exchange Membrane (PEM) Water Electrolyzers (PEMWE): Status, challenges and future needs. A mini review. *Electrochem. Commun.* **2020**, *114*, 106704. [[CrossRef](#)]

34. Corona-Guinto, J.L.; Cardeño-García, L.; Martínez-Casillas, D.C.; Sandoval-Pineda, J.M.; Tamayo-Meza, P.; Silva-Casarin, R.; González-Huerta, R.G. Performance of a PEM electrolyzer using RuIrCoOx electrocatalysts for the oxygen evolution electrode. *Int. J. Hydrogen Energy* **2013**, *38*, 12667–12673. [[CrossRef](#)]
35. Song, H.J.; Yoon, H.; Ju, B.; Kim, D.W. Highly Efficient Perovskite-Based Electrocatalysts for Water Oxidation in Acidic Environments: A Mini Review. *Adv. Energy Mater.* **2021**, *11*, 2002428. [[CrossRef](#)]
36. Lee, Y.; Suntivich, J.; May, K.J.; Perry, E.E.; Shao-Horn, Y. Synthesis and Activities of Rutile IrO<sub>2</sub> and RuO<sub>2</sub> Nanoparticles for Oxygen Evolution in Acid and Alkaline Solutions. *J. Phys. Chem. Lett.* **2012**, *3*, 399–404. [[CrossRef](#)] [[PubMed](#)]
37. Parra-Puerto, A.; Ng, K.L.; Fahy, K.; Goode, A.E.; Ryan, M.P.; Kucernak, A. Supported Transition Metal Phosphides: Activity Survey for HER, ORR, OER, and Corrosion Resistance in Acid and Alkaline Electrolytes. *ACS Catal.* **2019**, *9*, 11515–11529. [[CrossRef](#)]
38. Rojas, N.; Sanchez-Molina, M.; Sevilla, G.; Amores, E.; Almandoz, E.; Esparza, J.; Cruz Vivas, M.R.; Colominas, C. Coated stainless steels evaluation for bipolar plates in PEM water electrolysis conditions. *Int. J. Hydrogen Energy* **2021**, *46*, 25929–25943. [[CrossRef](#)]
39. Asri, N.F.; Husaini, T.; Sulong, A.B.; Majlan, E.H.; Daud, W.R.W. Coating of stainless steel and titanium bipolar plates for anticorrosion in PEMFC: A review. *Int. J. Hydrogen Energy* **2017**, *42*, 9135–9148. [[CrossRef](#)]
40. Wang, S.H.; Peng, J.; Lui, W.B. Surface modification and development of titanium bipolar plates for PEM fuel cells. *J. Power Sources* **2006**, *160*, 485–489. [[CrossRef](#)]
41. Ursúa, A.; Gandía, L.M.; Sanchis, P. Hydrogen production from water electrolysis: Current status and future trends. *Proc. IEEE* **2011**, *100*, 410–426. [[CrossRef](#)]
42. Ayers, K.E.; Anderson, E.B.; Capuano, C.; Carter, B.; Dalton, L.; Hanlon, G.; Manco, J.; Niedzwiecki, M. Research Advances towards Low Cost, High Efficiency PEM Electrolysis. *ECS Trans.* **2010**, *33*, 3–15. [[CrossRef](#)]
43. Shiva Kumar, S.; Himabindu, V. Hydrogen production by PEM water electrolysis—A review. *Mater. Sci. Energy Technol.* **2019**, *2*, 442–454. [[CrossRef](#)]
44. Chi, J.; Yu, H. Water electrolysis based on renewable energy for hydrogen production. *Chin. J. Catal.* **2018**, *39*, 390–394. [[CrossRef](#)]
45. Siva, T.; Rajkumar, S.; Muralidharan, S.; Sathiyarayanan, S. Bipolar properties of coatings to enhance the corrosion protection performance. *Prog. Org. Coat* **2019**, *137*, 105379. [[CrossRef](#)]
46. Dongfang, S.; Guixin, S.; Shanlong, P.; Dongdong, W.; Yue, L.; Heng, Z.; Xindong, W. Electrophoretic deposition of TiN coating on titanium bipolar plate used for PEM water electrolysis. *Electroplat. Finish.* **2022**, *41*, 497–505. [[CrossRef](#)]
47. Müller, A.; Kauranen, P.; von Ganski, A.; Hell, B. Injection moulding of graphite composite bipolar plates. *J. Power Sources* **2006**, *154*, 467–471. [[CrossRef](#)]
48. Ijaodola, O.; Ogungbemi, E.; Khatib, F.N.; Wilberforce, T.; Ramadan, M.; El Hassan, Z.; Thompson, J.; Olabi, A.G. Evaluating the Effect of Metal Bipolar Plate Coating on the Performance of Proton Exchange Membrane Fuel Cells. *Energies* **2018**, *11*, 3203. [[CrossRef](#)]
49. Ribeirinha, P.; Schuller, G.; Boaventura, M.; Mendes, A. Synergetic integration of a methanol steam reforming cell with a high temperature polymer electrolyte fuel cell. *Int. J. Hydrogen Energy* **2017**, *42*, 13902–13912. [[CrossRef](#)]
50. Stein, T.; Ein-Eli, Y. Challenges and Perspectives of Metal-Based Proton Exchange Membrane's Bipolar Plates: Exploring Durability and Longevity. *Energy Technol.* **2020**, *8*, 2000007. [[CrossRef](#)]
51. Stroebel, R. *Approach to Provide a Metallic Bipolar Plate Module to the Industry*; NADA: Woolloomooloo, NSW, Australia, 2017.
52. LaConti, A.B.; Griffith, A.E.; Croypley, C.C.; Kosek, J.A. Titanium Carbide Bipolar Plate for Electrochemical Devices. U.S. Patent 6083641, 1998.
53. Gago, A.; Ansar, A.; Wagner, N.; Arnold, J.; Friedrich, K.A. Titanium coatings deposited by thermal spraying for bipolar plates of PEM electrolyzers. In Proceedings of the 4th European PEFC and H<sub>2</sub> Forum, Lucerne, Switzerland, 2–5 July 2013.
54. Bi, J.; Yang, J.; Liu, X.; Wang, D.; Yang, Z.; Liu, G.; Wang, X. Development and evaluation of nitride coated titanium bipolar plates for PEM fuel cells. *Int. J. Hydrogen Energy* **2021**, *46*, 1144–1154. [[CrossRef](#)]
55. Barrera, O.; Bombac, D.; Chen, Y.; Daff, T.D.; Galindo-Nava, E.; Gong, P.; Haley, D.; Horton, R.; Katzarov, I.; Kermod, J.R.; et al. Understanding and mitigating hydrogen embrittlement of steels: A review of experimental, modelling and design progress from atomistic to continuum. *J. Mater. Sci.* **2018**, *53*, 6251–6290. [[CrossRef](#)] [[PubMed](#)]
56. Yang, C.J.; Liang, C.H.; Wang, H. Hydrogen embrittlement of titanium and its alloys. *Corros. Sci. Prot. Technol.* **1970**, *18*, 561–576.
57. Li, Y.S.; Zhang, C.Z.; Ma, H.T.; Yang, L.Z.; Zhang, L.L.; Tang, Y.; Li, X.J.; He, L.L.; Feng, R.; Yang, Q.; et al. CVD nanocrystalline diamond coatings on Ti alloy: A synchrotron-assisted interfacial investigation. *Mater. Chem. Phys.* **2012**, *134*, 145–152. [[CrossRef](#)]
58. Hu, X.; Xu, D.; Byun, T.S.; Wirth, B.D. Modeling of irradiation hardening of iron after low-dose and low-temperature neutron irradiation. *Model. Simul. Mat. Sci. Eng.* **2014**, *22*, 065002. [[CrossRef](#)]
59. Liu, G.; Peng, S.; Hou, F.; Fang, B.; Wang, X. Au-TiO<sub>2</sub>/Ti Hybrid Coating as a Liquid and Gas Diffusion Layer with Improved Performance and Stability in Proton Exchange Membrane Water Electrolyzer. *Molecules* **2022**, *27*, 6644. [[CrossRef](#)] [[PubMed](#)]
60. Lædre, S.; Kongstein, O.E.; Oedegaard, A.; Karoliussen, H.; Seland, F. Materials for Proton Exchange Membrane water electrolyzer bipolar plates. *Int. J. Hydrogen Energy* **2017**, *42*, 2713–2723. [[CrossRef](#)]
61. Joseph, S.; McClure, J.C.; Chianelli, R.; Pich, P.; Sebastian, P.J. Conducting polymer-coated stainless steel bipolar plates for proton exchange membrane fuel cells (PEMFC). *Int. J. Hydrogen Energy* **2005**, *30*, 1339–1344. [[CrossRef](#)]
62. Wang, S.H.; Peng, J.; Lui, W.B.; Zhang, J.S. Performance of the gold-plated titanium bipolar plates for the light weight PEM fuel cells. *J. Power Sources* **2006**, *162*, 486–491. [[CrossRef](#)]

63. Song, S.H.; Min, B.K.; Hong, M.-H.; Kwon, T.-Y. Application of a novel CVD TiN coating on a biomedical Co–Cr Alloy: An evaluation of coating layer and substrate characteristics. *Materials* **2020**, *13*, 1145. [[CrossRef](#)]
64. Jin, N.; Yang, Y.; Luo, X.; Xia, Z. Development of CVD Ti-containing films. *Prog. Mater. Sci.* **2013**, *58*, 1490–1533. [[CrossRef](#)]
65. Aliofkhaezrai, M.; Ali, N. PVD Technology in Fabrication of Micro- and Nanostructured Coatings. *Compr. Mater. Process.* **2014**, *7*, 49–84.
66. Mansoor, N.S.; Fattah-alhosseini, A.; Elmkhah, H.; Shishehian, A. Comparison of the mechanical properties and electrochemical behavior of TiN and CrN single-layer and CrN/TiN multi-layer coatings deposited by PVD method on a dental alloy. *Mater. Res. Express* **2020**, *6*, 126433. [[CrossRef](#)]
67. Li, P.; Ding, X.; Yang, Z.; Chen, M.; Wang, M.; Wang, X. Electrochemical synthesis and characterization of polyaniline-coated PEMFC metal bipolar plates with improved corrosion resistance. *Ionics* **2018**, *24*, 1129–1137. [[CrossRef](#)]
68. Wang, Y.; Northwood, D.O. An investigation into polypyrrole-coated 316L stainless steel as a bipolar plate material for PEM fuel cells. *J. Power Sources* **2006**, *163*, 500–508. [[CrossRef](#)]
69. Zhang, T.; Zeng, C.L. Corrosion protection of 1Cr18Ni9Ti stainless steel by polypyrrole coatings in HCl aqueous solution. *Electrochim. Acta* **2005**, *50*, 4721–4727. [[CrossRef](#)]
70. García, M.A.L.; Smit, M.A. Study of electrodeposited polypyrrole coatings for the corrosion protection of stainless steel bipolar plates for the PEM fuel cell. *J. Power Sources* **2006**, *158*, 397–402. [[CrossRef](#)]
71. Deyab, M.A. Corrosion protection of aluminum bipolar plates with polyaniline coating containing carbon nanotubes in acidic medium inside the polymer electrolyte membrane fuel cell. *J. Power Sources* **2014**, *268*, 50–55. [[CrossRef](#)]
72. Joseph, S.; McClure, J.C.; Sebastian, P.J.; Moreira, J.; Valenzuela, E. Polyaniline and polypyrrole coatings on aluminum for PEM fuel cell bipolar plates. *J. Power Sources* **2008**, *177*, 161–166. [[CrossRef](#)]
73. Chen, W.C.; Lo, Y.; Chen, H.S. Effects of Ti surface treatments with silane and arginylglycylaspartic acid peptide on bone cell progenitors. *Odontology* **2014**, *103*, 322–332. [[CrossRef](#)]
74. Deflorian, F.; Rossi, S.; Fedrizzi, L. Silane pre-treatments on copper and aluminium. *Electrochim. Acta* **2006**, *51*, 6097–6103. [[CrossRef](#)]
75. Ciešlik, M.; Engvall, K.; Pan, J.; Kotarba, A. Silane–parylene coating for improving corrosion resistance of stainless steel 316L implant material. *Corros. Sci.* **2011**, *53*, 296–301. [[CrossRef](#)]
76. Fedel, M.; Olivier, M.; Poelman, M.; Deflorian, F.; Rossi, S.; Druart, M.E. Corrosion protection properties of silane pre-treated powder coated galvanized steel. *Prog. Org. Coat* **2009**, *66*, 118–128. [[CrossRef](#)]
77. Edzatty, A.N.; Norzilah, A.H.; Jamaludin, S.B. Preliminary study: Direct growth carbon nanomaterials on metal substrate to improve corrosion resistance. *Mater. Sci. Forum* **2015**, *819*, 81–86. [[CrossRef](#)]
78. Li, H.; Wang, R.; Hu, H.; Liu, W. Surface modification of self-healing poly(urea-formaldehyde) microcapsules using silane-coupling agent. *Appl. Surf. Sci.* **2008**, *255*, 1894–1900. [[CrossRef](#)]
79. Ma, Z.; Zhu, F.; Zhao, T. Effects of surface modification of silane coupling agent on the properties of concrete with freeze-thaw damage. *KSCE J. Civ. Eng.* **2017**, *22*, 657–669. [[CrossRef](#)]
80. Rashno, A.; Mohebi Damabi, R.; Rezaee Niaraki, P.; Ahmadi, S. A new amino silane coupling agent for old corrugated container fibers/high density polyethylene composites. *Polym. Compos.* **2018**, *39*, 2054–2064. [[CrossRef](#)]
81. Ge, M.; Wang, X.; Du, M.; Liang, G.; Hu, G.; SM, J.A. Effects on the Mechanical Properties of Nacre-Like Bio-Hybrid Membranes with Inter-Penetrating Petal Structure Based on Magadiite. *Materials* **2019**, *12*, 173. [[CrossRef](#)]
82. Ren, Y.; Zhou, Q. Study on silane treatment technology in the painting pretreatment. *Adv. Mat. Res.* **2012**, *482–484*, 1192–1195. [[CrossRef](#)]
83. Wessling, B. Corrosion prevention with an organic metal (polyaniline): Surface ennobling, passivation, corrosion test results. *Mater. Corros.* **1996**, *47*, 439–445. [[CrossRef](#)]
84. Deyab, M.A.; Mele, G. Stainless steel bipolar plate coated with polyaniline/Zn-Porphyrin composites coatings for proton exchange membrane fuel cell. *Sci. Rep.* **2020**, *10*, 3277. [[CrossRef](#)]
85. Cooper, L.; El-Kharouf, A. Titanium Nitride Polyaniline Bilayer Coating for Metallic Bipolar Plates used in Polymer Electrolyte Fuel Cells. *Fuel Cells* **2020**, *20*, 453–460. [[CrossRef](#)]
86. Jiang, L.; Syed, J.A.; Lu, H.; Meng, X. In-situ electrodeposition of conductive polypyrrole-graphene oxide composite coating for corrosion protection of 304SS bipolar plates. *J. Alloys Compd.* **2019**, *770*, 35–47. [[CrossRef](#)]
87. Abu-Thabit, N.Y.; Makhoulouf, A.S.H. Recent advances in polyaniline (PANI)-based organic coatings for corrosion protection. *Handb. Smart Coat. Mater. Prot.* **2014**, *2014*, 459–486. [[CrossRef](#)]
88. MA, C.; SG, P.; PR, G.; Shashwati, S.; VB, P. Synthesis and Characterization of Polypyrrole (PPy) Thin Films. *Soft Nanosci. Lett.* **2011**, *1*, 6–10.
89. Liu, S.; Pan, T.J.; Wang, R.F.; Yue, Y.; Shen, J. Anti-corrosion and conductivity of the electrodeposited graphene/polypyrrole composite coating for metallic bipolar plates. *Prog. Org. Coat* **2019**, *136*, 105237. [[CrossRef](#)]
90. Jiang, L.; Syed, J.A.; Gao, Y.; Zhang, Q.; Zhao, J.; Lu, H.; Meng, X. Electropolymerization of camphorsulfonic acid doped conductive polypyrrole anti-corrosive coating for 304SS bipolar plates. *Appl. Surf. Sci.* **2017**, *426*, 87–98. [[CrossRef](#)]
91. Sun, Y.; Hu, C.; Cui, J.; Shen, S.; Qiu, H.; Li, J. Electrodeposition of polypyrrole coatings doped by benzenesulfonic acid-modified graphene oxide on metallic bipolar plates. *Prog. Org. Coat* **2022**, *170*, 106995. [[CrossRef](#)]

92. Yan, S.; Song, H.; Li, Y.; Yang, J.; Jia, X.; Wang, S.; Yang, X. Integrated reduced graphene oxide/polypyrrole hybrid aerogels for simultaneous photocatalytic decontamination and water evaporation. *Appl. Catal. B* **2022**, *301*, 120820. [[CrossRef](#)]
93. Tan, Q.; Wang, Y. Preparation and performances of modified Ti<sub>4</sub>O<sub>7</sub> doped polypyrrole coating for metallic bipolar plates. *Corros. Sci.* **2021**, *190*, 109703. [[CrossRef](#)]
94. Akula, S.; Kalaiselvi, P.; Sahu, A.K.; Chellammal, S. Electrodeposition of conductive PAMT/PPY bilayer composite coatings on 316L stainless steel plate for PEMFC application. *Int. J. Hydrogen Energy* **2021**, *46*, 17909–17921. [[CrossRef](#)]
95. He, J.; Zeng, W.; Shi, M.; Lv, X.; Fan, H.; Lei, Z. Influence of expandable graphite on flame retardancy and thermal stability property of unsaturated polyester resins/organic magnesium hydroxide composites. *J. Appl. Polym. Sci.* **2020**, *137*, 47881. [[CrossRef](#)]
96. Oleksy, M.; Oliwa, R.; Heneczkowski, M.; Mossety-Leszczak, B.; Galina, H.; Budzik, G. Composites of epoxy resin with modified bentonites for aviation industry. *Polimery* **2012**, *57*, 228–235. [[CrossRef](#)]
97. Luo, B.; Wang, X.; Zhao, Q.; Li, L. Synthesis, characterization and dielectric properties of surface functionalized ferroelectric ceramic/epoxy resin composites with high dielectric permittivity. *Compos. Sci. Technol.* **2015**, *112*, 1–7. [[CrossRef](#)]
98. Abdullah, S.I.; Ansari, M.N.M. Mechanical properties of graphene oxide (GO)/epoxy composites. *HBRC J.* **2015**, *11*, 151–156. [[CrossRef](#)]
99. Luo, B.; Wang, X.; Zhao, Q.; Li, L. A study of the effects of the matrix epoxy resin and graphene oxide (GO) manufacturing process on the tensile behaviour of GO-epoxy nanocomposites. *Plast. Rubber Compos.* **2017**, *46*, 405–412.
100. Luo, B.; Wang, X.; Tian, E.; Song, H.; Li, L. Interfacial electronic and structural properties of SiO<sub>2</sub>(010)/BaTiO<sub>3</sub>(001) from first-principles calculations. *Ceramics International.* **2017**, *43*, 12988–12991. [[CrossRef](#)]
101. Sun, M.Y.; Jiang, H.T.; Shi, B.; Zhou, G.Y.; Inyang, H.I.; Feng, C.X. Development of FBG salinity sensor coated with lamellar polyimide and experimental study on salinity measurement of gravel aquifer. *Measurement* **2019**, *140*, 526–537. [[CrossRef](#)]
102. Liu, B.D.; Li, D.S.; Yang, J.H. The Research on Sacrificial Layer in the Fabrication of Micro Electromagnetic Relay. *AMR.* **2009**, *60–61*, 160–164. [[CrossRef](#)]
103. Zhu, G.; Hou, J.; Zhu, H.; Qiu, R.; Xu, J. Electrochemical synthesis of poly(3,4-ethylenedioxythiophene) on stainless steel and its corrosion inhibition performance. *J. Coat Technol. Res.* **2013**, *10*, 659–668. [[CrossRef](#)]
104. Jia, Y.K.; Chen, P.; Zhang, Q.H.; Sun, J. Thermal Reduced Graphene Oxide/Polyimide Nanocomposite Coating: Fabrication and Anticorrosive Property. *Wuji Cailiao Xuebao/J. Inorg. Mater.* **2017**, *32*, 1257–1263.
105. Liu, Y.; Min, L.; Zhang, W.; Wang, Y. High-performance graphene coating on titanium bipolar plates in fuel cells via cathodic electrophoretic deposition. *Coatings* **2021**, *11*, 437. [[CrossRef](#)]
106. Lee, D.; Lee, E.; Yoon, J.; Keith, B.; Oh, T.; Woo, S.P.; Yoon, Y.S.; Kim, D.J. Electrophoretic Deposition of Titanium Nitride Onto 316 Stainless Steel As a Bipolar Plate for Fuel Cell Application. *ECS Trans.* **2017**, *80*, 851. [[CrossRef](#)]
107. Liu, Y.; Huang, S.; Peng, S.; Zhang, H.; Wang, L.; Wang, X. Novel Au nanoparticles-inlaid titanium paper for PEM water electrolysis with enhanced interfacial electrical conductivity. *Int. J. Miner. Metall. Mater.* **2022**, *29*, 1090–1098. [[CrossRef](#)]
108. Hermann, A.; Chaudhuri, T.; Spagnol, P. Bipolar plates for PEM fuel cells: A review. *Int. J. Hydrogen Energy* **2005**, *30*, 1297–1302. [[CrossRef](#)]
109. Song, Y.; Zhang, C.; Ling, C.Y.; Han, M.; Yong, R.Y.; Sun, D.; Chen, J. Review on current research of materials, fabrication and application for bipolar plate in proton exchange membrane fuel cell. *Int. J. Hydrogen Energy* **2020**, *45*, 29832–29847. [[CrossRef](#)]

**Disclaimer/Publisher’s Note:** The statements, opinions and data contained in all publications are solely those of the individual author(s) and contributor(s) and not of MDPI and/or the editor(s). MDPI and/or the editor(s) disclaim responsibility for any injury to people or property resulting from any ideas, methods, instructions or products referred to in the content.